Surface-Induced Microphase Separation in Spin-Cast Ultrathin Diblock Copolymer Films on Silicon Substrate before and after Annealing

Elke Buck and Jürgen Fuhrmann*

Institute of Physical Chemistry, Technical University Clausthal, Arnold-Sommerfeld-Str. 4, D-38678 Clausthal-Zellerfeld, Germany

Received July 24, 2000

ABSTRACT: The microphase structures of ultrathin symmetric polystyrene/poly(methyl methacrylate) diblock copolymer films on silicon substrate under variation of film thicknesses in the nanometer range were investigated by using AFM. The microphases were identified by simultaneously measuring the topography and the phase-shift image in TappingMode and by comparing the results with the topography after selectively etching the poly(methyl methacrylate) phase. The thinnest spin-cast film showing complete wetting was only 1.8 nm thick. However, even for this film a microphase separation in the range of the correlation length (L) of the diblock bulk material was observed. For this minimum film thickness, the calculated PMMA microdomain volume approaches the volume of a single PMMA coil, which may be discussed as the limiting microdomain volume necessary as a critical wetting condition. Geometrical considerations lead to an average PMMA/silicon substrate contact angle of 46° in the spin-cast and vacuum-dried ultrathin diblock copolymer films. Annealing of these films at 130 °C reveals a second minimum thickness, at which the microphases show coplanar lamellar ordering with the PMMA at the substrate and the PS at the surface. This minimum thickness of coplanar ordering is about 40% higher than the calculated width of the interface between PS and PMMA in the bulk.

Introduction

Microphase separation and microdomain morphology in thin films of symmetric polystyrene/poly(methyl methacrylate) diblock copolymers (P(S-*b*-MMA)) have been investigated intensively during the past decade. The results, which are reviewed in a series of articles,[1−12] demonstrate that the most-observed film structure is the parallel ordering of the lamellae with respect to the interface and that this orientation is controlled by surface and interface energies in the equilibrium state. This parallel alignment of the lamellae depends ideally on the quantization of the film thickness; i.e., thicknesses corresponding to integer or half-integer multiples of the lamellar period (L) can be observed in layered order on the substrate. If the mean film thickness is not exactly a given number of periods, islands or holes of height or depth L at the free surface were formed to accommodate the layered microphase morphology.[2,5] In films with thicknesses between $3L/2$ and $L/4$ the thicknesses of the PS and PMMA layers and the width of the interface between the layers were found to vary with film thickness.[10]

In this report we focus on the film morphology of ultrathin symmetric P(S-*b*-MMA) diblock copolymer films on silicon substrate after spin-coating of a highly diluted toluene solution and after subsequent annealing above the glass-transition temperature of both polymer blocks. In this case, ultrathin means film thicknesses of only a few nanometers, i.e., far below $L/2$. Hence, we investigate nanostructures in the ultrathin film by inspecting the polymer/air interface by AFM methods.

To vary the film thickness of the diblock copolymer films, we have chosen two parameters for its control: polymer concentration of the solution droplet used for spin-coating and rotation speed of the substrate. The amount of solution and temperature were kept constant. In this way, we were able to prepare even the thinnest-closed diblock copolymer film.

The so-prepared ultrathin samples were subsequently annealed in order to determine the temperature-dependent morphological changes which should be a compromise between the amount of material, minimal surface, and interface energies as well as stresses of the block copolymer chains.

For the investigations of microphase structures in ultrathin diblock copolymer films, AFM techniques are suitable methods giving three-dimensional information with high resolution of both height and material contrast.

We therefore used AFM TappingMode, recording height and phase shift simultaneously.

We have chosen the TappingMode parameters for light-tapping,[13] so the contrast of phase shift is given by differences in attractive forces between the tip and the two components at the surface.

A further topographical contrast revealing the morphology can be produced by selectively degradation the PMMA microphases in air plasma.[14−17] Combining the contrast of TappingMode phase imaging with the topography after selective etching allows us to identify the two different components PS and PMMA.

Experimental Section

Diblock Copolymer. The symmetric diblock copolymer P(S-*b*-MMA), courtesy of R. Stadler, is described elsewhere.[18] The molecular weights of the styrene and the methyl methacrylate blocks are 128 and 147 kg/mol, respectively; $M_w/M_n = 1.11$ and it is denoted as SM120. Its weight fraction measured by ^{1}H NMR amounts to $w_{PS} = 0.4$. For the identification of the microphases (Figure 1) a second diblock copolymer (SM78) was used, having molecular weights of the styrene and the methyl methacrylate blocks of 78 and 77 kg/mol, respectively; $M_w/M_n = 1.09$ and $w_{PS} = 0.47$.

* To whom correspondence should be addressed. Tel +49 5323 72 2205; Fax +49 5323 72 2863; E-mail fuhrmann@pc.tu-clausthal.de.

10.1021/ma001288f CCC: $20.00
Published on Web 03/02/2001

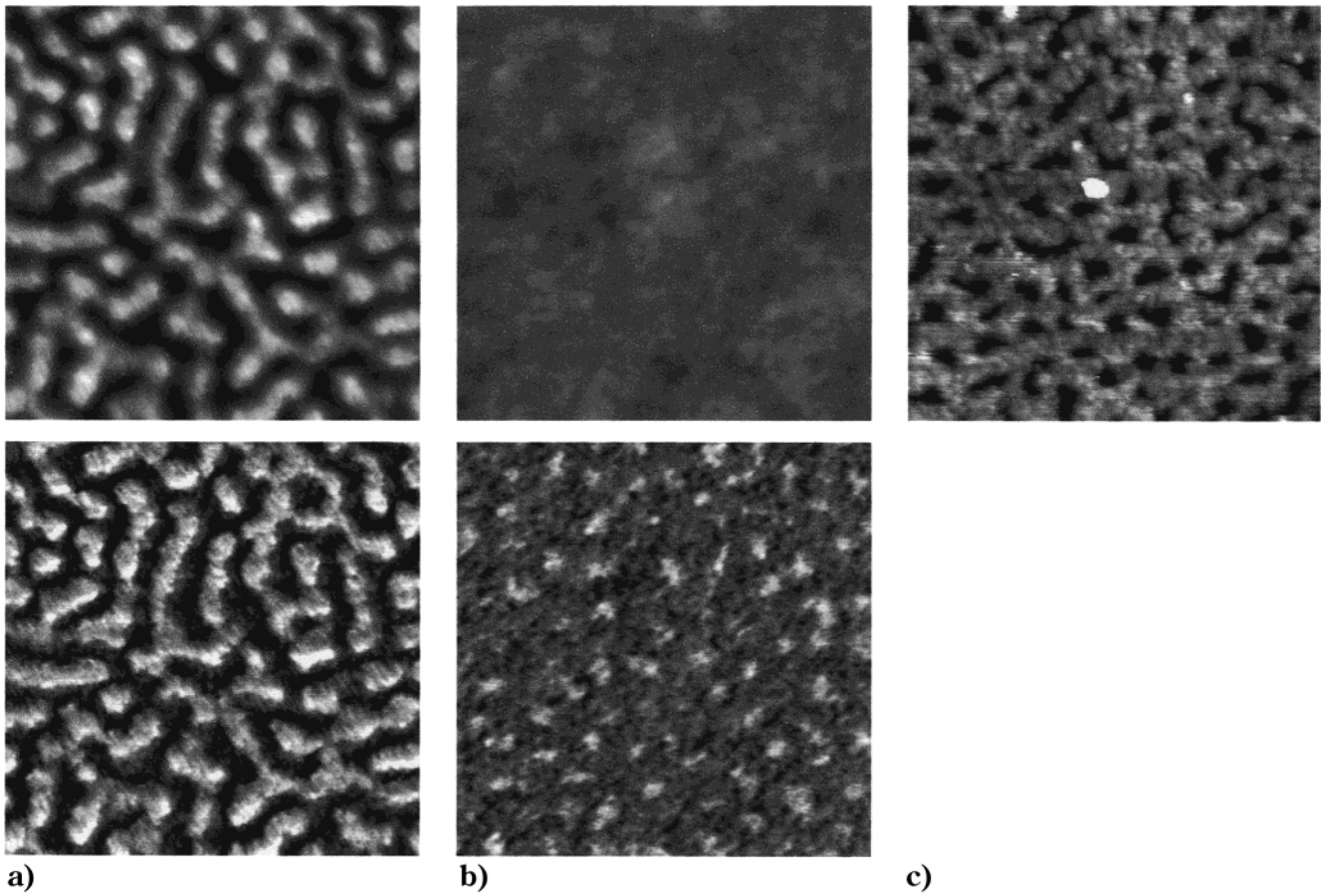

Figure 1. Topography (top) and phase contrast (bottom) of a spin-cast (<100 rpm) P(S-*b*-MMA) diblock copolymer film on silicon substrate, using 0.5 g/L SM78 in toluene. Image size: 500 nm × 500 nm each (a) after vacuum-drying at 50 °C (height: 8 nm, phase shift: 25°); (b) after annealing 4 h at 140 °C (height: 8 nm, phase shift: 10°); (c) after selectively etching the PMMA block of the annealed film (topography only, height: 10 nm).

Sample Preparation. The copolymer films were prepared by spin-coating 5 μL of a toluene solution with various concentrations (0.25, 0.5, 1.5, 2.5, and 3.5 g/L) at room temperature and standard pressure onto polished silicon at 4500 and 10 500 rpm, respectively. The SM78 film in Figure 1 is prepared at about 100 rpm with a polymer concentration of 0.5 g/L.

The substrate (about 5 mm × 5 mm) was cut from a polished silicon wafer, cleaned with a precision wipe and with air plasma at 100 W for 1 min.

In contrast to the standard spin-coating procedure where the solution is positioned onto the substrate and then rotation is started, the solution was dropped onto the already-rotating substrate; in this manner the whole solution reaches the rotating substrate in one droplet. The substrate was held in rotation for one more minute. All spin-cast films were dried in a vacuum for 4 h at 50 °C.

To investigate the thermal equilibrium of the thickness-constrained ultrathin films, the samples were annealed at standard pressure in steps of 10 °C, starting at 60 °C and ending at 160 °C for at least 24 h at each step. Topography and phase contrast were measured after cooling to room temperature.

Selective Etching. The plasma cleaning of the substrate and the sample etching were performed in a Haarick (PDC-32G) plasma cleaner. For substrate cleaning a power of 100 W was used for about 1 min. For selective etching the PMMA microphases, a power of 40 W was used in steps of 5 s.

The air plasma was regulated by controlling the air pressure to obtain the brightest plasma luminosity. After each etching period the samples were kept in a vacuum for an additional 15 min.

Atomic Force Microscopy. The AFM measurements presented in this paper were all made by a MultiMode scanning probe microscope, NanoScope III, Digital Instruments. We used TappingMode silicon cantilevers with a cantilever length of 125 μm (Nanosensors). All pictures were taken with light tapping[13] ($A_0 \approx 70$ nm; $r_{sp} > 0.8$).

All images presented here were taken from an area located 1 mm around the rotational axis given in the spin-coating process.

The analysis of the AFM images was made with the following programs: roughness in the Nanoscope software *Analyze/Roughness*; periodicity in the Nanoscope software *Modify/2D Spectrum*; microphase fractions in the Nanoscope software combining *Analyze/Grain Size* and *Analyze/Bearing* (analyzing the image and the inverted image to minimize the error coming from visualizing colors); the number of PMMA microphases per area was evaluated in the DATA TRANSLATION software GLOBAL LAB IMAGE.

A. Lippitz and W. Unger (Federal Institute for Materials Research and Testing) kindly measured the film thicknesses by ESCA from the intensity quotient of carbon and silicon taking different takeoff angles (20°, 40°, 60°).

The thicknesses of the two thinnest films were measured by AFM, scratching a hole in the layer by applying a high force in contact mode between tip and sample and followed by scanning the hole with moderate force in TappingMode. The resulting holes were about 100 nm in diameter. The images from which the depth were taken were 4 μm^2.

H. Sturm (Federal Institute for Materials Research and Testing) kindly measured the two films: film **f** (Table 1) after annealing and film **a** (Table 1) after annealing and subsequent etching by harmonically modulated friction (HM-LFM) by using silicon cantilevers with a cantilever length of 450 μm (Nanosensors). The experimental details of this AFM method are described elsewhere.[19,20]

Table 1[a]

film	v [rpm]	c [g/L]	$\langle h \rangle$ [nm]	R_a [nm]	F^u_{PMMA}	periodicity [nm]	H [1/μm^2]
		0.25	incomplete wetting				
a	4500	0.5	2.1	0.4	0.43	78	239
b		1.5	5.8	0.5	0.43	72	224
c		2.5	7.8	0.72	0.41	76	197
d		3.5	9.7	1.19	0.47	77	76
e		0.5	1.8	0.35	0.42	83	240
f	10500	1.5	4.6	0.41	0.46	76	215
g		2.5	5.8	0.54	0.43	67	193
h		3.5	7.8	0.75	0.41	71	147

[a] v := rotation speed; c := polymer concentration; $\langle h \rangle$:= film thickness measured by ESCA; R_a := film roughness; F^u_{PMMA} := microphase fraction of PMMA at the surface; H := number of PMMA microphases per area.

Results and Discussion

Microphase Identification. For the investigation of the morphology of ultrathin diblock copolymer films, it is essential to clearly identify the individual microphases of polystyrene and poly(methyl methacrylate). To do so, all films were measured by atomic force microscopy, using TappingMode at light tapping[13] while simultaneously recording the phase shift of the cantilever oscillation.

The height and phase shift of a spin-cast film of SM78 on silicon substrate are shown in Figure 1a. Both topography and phase contrast show wormlike structures. The elevated structures show a brighter contrast in the phase-shift image. Topography and microphase morphology thus correlate in the spin-cast film.

Figure 1b shows the same film after annealing for 4 h at 140 °C. It should be noted that the annealing process is not completed yet, and hence an interesting snapshot of the ongoing annealing process is shown. The surface is completely smoothed out, and the wormlike structures of the film surface have disappeared due to the annealing procedure. But in the image of phase shift, there are still two phases with distinguishing features: bright round domains in a dark continuous matrix. The bright domains have a diameter of about 27 nm and a periodicity of about 53 nm; both values are comparable to the lamellar periodicity of 50 nm as theoretically predicted for the bulk diblock SM78.[21]

Figure 1c shows the topography of this snapshot after selectively etching the PMMA phase. The etching procedure generates round holes of about 26 nm in diameter with a periodicity of about 53 nm. These values are in good agreement with the results obtained from Figure 1b. It should be noted that the etching procedure is chosen appropriately so that the microphase organization of the polystyrene block is nearly unaffected, and it remains as a continuous, network-like structure.

This result points out that the phase shift contrasts the microphases in the manner that PMMA appears brighter than PS, even in the case of a topographically flat film (see Figure 1b). Again, this contrast (only a few degrees) is found only at light tapping;[13] its reason could be the differences in adhesion between the silicon cantilever and PS and PMMA.

The PMMA microphases in the as-cast film surfaces are higher than the PS microphases, but the latter appear as continuous phase as can be seen from Figure 1 a. This morphological phenomenon of spin-cast films is examined systematically by making use of a concentration series finding the thinnest possible film and the evolution to thicker films.

Minimum Thickness of Spin-Cast Films. To find the minimum film thickness of complete wetting, a concentration series of SM120 in toluene were spin-coated onto silicon substrate rotating at two different speeds. The topography of the resulting films, prepared at 4500 rpm and measured by AFM, is shown in the top portion of Figure 2. In the lower portion of Figure 2 the image of phase shift is shown, revealing the morphology of the film.

The results of the quantitative analysis with the film thicknesses measured by ESCA are given in Table 1. All quantitative results were taken from images of 1 μm^2, by analyzing the roughness R_a from the topography and the others (periodicity, microphase surface fraction F^u_{PMMA}, and number H of PMMA microphases per area) from the image of phase shift.

A polymer concentration of 0.25 g/L of SM120 leads to incomplete wetting of the silicon substrate at both rotation speeds.

It is clearly seen that both the periodicity and microphase surface fraction do not show a systematic trend. The average of the periodicity is 75 nm and is only slightly higher than the calculated $L = 70$ nm of the bulk material for SM120.[21] The average of the microphase surface fraction of PMMA at the surface is 43%, hence taking the smaller portion of the total surface. The roughness and the number of PMMA microphases per unit area are shown graphically in parts a and b of Figure 3, respectively.

The number of PMMA microphases per unit area increases with decreasing film thickness, while the roughness decreases. By approaching the thinnest possible film, both the number of PMMA microphases per unit area and the roughness asymptotically approach a maximum and minimum value, respectively.

The PMMA volume fraction φ_{PMMA} of 57.4% in the diblock copolymer SM120 was calculated from the PMMA weight fraction ($w_{PMMA} = 0.6$) using the bulk densities of the two polymers ($\rho_{PS} = 1.05$ kg/L; $\rho_{PMMA} = 1.17$ kg/L).[22]

Neglecting any substrate-induced density phenomena as predicted by Baschnagel and Binder[23] and assuming the interfaces between PS and PMMA standing perpendicular to the silicon substrate (Figure 4, top), the PMMA volume fraction f_{PMMA} of the ultrathin films can be calculated from the measured surface fractions (Table 1) in consideration of the film roughness, which is predominantly caused by the microphase morphology (cf. Figure 2):

$$f_{PMMA} = \frac{F^u_{PMMA}(d + R_a)}{F^u_{PMMA}(d + R_a) + F^u_{PS}(d - R_a)} \qquad (1)$$

For the investigated ultrathin films a mean value of 49.5% is obtained. A reasonable explanation for the noticeable difference between the calculated volume

Table 2[a]

film	h_{PMMA} [nm]	A^u [nm]	V_{PMMA} [nm^3]	A^l [nm^2]	F^l_{PMMA}	α [deg]
a	2.50	1800	5 040	2240	0.54	41
b	6.30	1930	14 860	2820	0.63	48
c	8.52	2060	22 730	3330	0.66	48
d	19.89	6170	73 260	7300	0.56	57
e	2.15	1730	4 305	2290	0.55	31
f	5.01	2130	12 280	2790	0.60	50
g	6.34	2230	17 250	3250	0.63	47
h	8.55	2760	30 460	4440	0.65	45

[a] h_{PMMA} := height of the PMMA microphases ($h_{PMMA} = \langle h \rangle + R_a$); A^u := upper area of a truncated cone of PMMA ($A^u = F^u_{PMMA}/H$); V_{PMMA} := volume of a truncated cone of PMMA ($\varphi_{PMMA}\langle h \rangle/H$); A^l := lower area of a truncated cone of PMMA; F^l_{PMMA} := fraction of silicon surface covered by PMMA; α := PMMA/silicon substrate contact angle (from eq 3).

fraction f_{PMMA} and the bulk volume fraction φ_{PMMA} is a PMMA/silicon substrate contact angle smaller than 90°, which is frozen in during the spin-coating and drying process (Figure 4, bottom).

Assuming the microphases as irregular truncated cones with bulk density and neglecting the volume of the PS/PMMA interface, the area at the silicon substrate covered by PMMA as well as an average PMMA/substrate contact angle can be calculated.

The volume V_{PMMA} of an irregular truncated PMMA cone is

$$V_{PMMA} = \frac{h_{PMMA}}{3}(A^u + \sqrt{A^u A^l} + A^l) \qquad (2)$$

h_{PMMA} is the height of the PMMA microphase and A^u is the upper area of the truncated cone, corresponding to the average area of a PMMA microphase measured by AFM. A^l, the lower area of this truncated cone, can be obtained by calculating the volume V_{PMMA} for an average PMMA microphase considering the PMMA volume fraction φ_{PMMA}. Table 2 shows the results for each of the eight films. By multiplying A^l with the number H of PMMA microphases per area, the fraction of silicon surface covered by PMMA, F^l_{PMMA}, is obtained. The mean value of F^l_{PMMA} is 60%.

In the case of centered truncated cones the PMMA/silicon substrate contact angle α is

$$\tan \alpha = \frac{h_{PMMA}}{\left(\sqrt{\frac{A^l}{\pi}} - \sqrt{\frac{A^u}{\pi}}\right)} \qquad (3)$$

The results are given in Table 2. The mean value of this contact angle α is 46°.

For these calculations it has to be noted that possible deviations from the bulk densities[23] of the two polymers might lead to a reduction of the substrate coverage by PMMA and of the tilt of the PS/PMMA interface.

The topography of the as-cast film (Figures 1a and 2), contradicting with its elevated PMMA microdomains any isothermal isobaric minimal surface energy considerations, can be explained by inspecting the solution from which the diblock copolymer is spin-cast: Han and Mozer[24] showed for a diluted solution of a PS−PMMA diblockcopolymer in toluene that the PMMA chains are under Θ-condition whereas the PS chains are slightly swollen. Therefore, the toluene is a selectively good solvent for the PS block and a poor solvent for PMMA block of the diblock copolymer. This may be the reason for the higher shrinkage of the PS block relative to the PMMA block in the film formation process.

The whole process of spin-coating the toluene/diblock copolymer solution takes not more than 2 s from spreading up to film formation. In this time two nonseparable events have to occur simultaneously: adhesion of the polymer chains to the substrate and microphase formation. It is important to note that for the microphase formation several polymer chains of the same type (i.e., PS or PMMA) have to aggregate.

The described process of film formation is therefore a substrate-supported decomposition. The question cannot be solved yet whether the substrate represents the nucleus for binodal decomposition or the adhesion between silicon and premature precipitated PMMA causes the film morphology and topography.

The measured topography is not developed before drying in a vacuum at 50 °C. During the drying procedure, the solvent evaporates from the immobile microphases, and shrinking occurs only in the direction normal to the silicon surface causing shear stress. PS microphases collapse more than the PMMA phases, because the toluene content in the PS-rich microdomains is higher.

In summary, the structuring of spin-cast ultrathin diblock copolymer films emerges from the formation of laterally fixed microphases during the spin-coating process as well as from differences of the two components swelling in solution and then collapsing during the drying process.

In the following we want to derive a criterion for the lower limit of film stability by inspecting the thinnest film **e**. Film **e** is only 1.8 nm thick and shows, as all other films, a periodicity in the range of L for the SM120. The derivation of the criterion for the lower limit of film stability is done by comparing the average volume of a PMMA microdomain in film **e** with the volume of the PMMA chain under Θ-condition. The radius of gyration of a homopolymer chain (under Θ-condition) with the same degree of polymerization as the PMMA block in the used SM120 ($N = 1470$) is 8.6 nm.[22] The volume of a sphere with this radius is thus 2664 nm^3.

Assuming bulk densities of the two polymers, the calculated PMMA microdomain volume in film **e** is 4305 nm^3 (Table 2).

The ratio of an average PMMA microdomain volume in film **e** and the volume of a single PMMA chain under Θ-condition is 1.6. This leads to the following conclusion: To reach complete wetting of the silicon substrate in ultrathin diblock copolymer films, the average volume of the PMMA microphases must be slightly higher than the volume of a single PMMA chain under Θ-condition.

Coplanar Ordering Limit. The eight spin-cast films given in Table 1 were annealed to investigate the thickness-dependent morphological changes and mobility in ultrathin diblock copolymer films due to temperature treatments.

After annealing at 100 °C, the thinnest film **e** (1.8 nm) has completely changed its morphlogy. Film **a** (2.1 nm) has changed its morphology after annealing at 110 °C and film **f** (4.6 nm) at 120 °C. The thicker films (>5.8 nm) changed their morphology after annealing at 130 °C. Annealing all samples up to 160 °C did not reveal any further structural changes.

A selection of the topographical images of the resulting films is shown in Figure 5. The topography of the

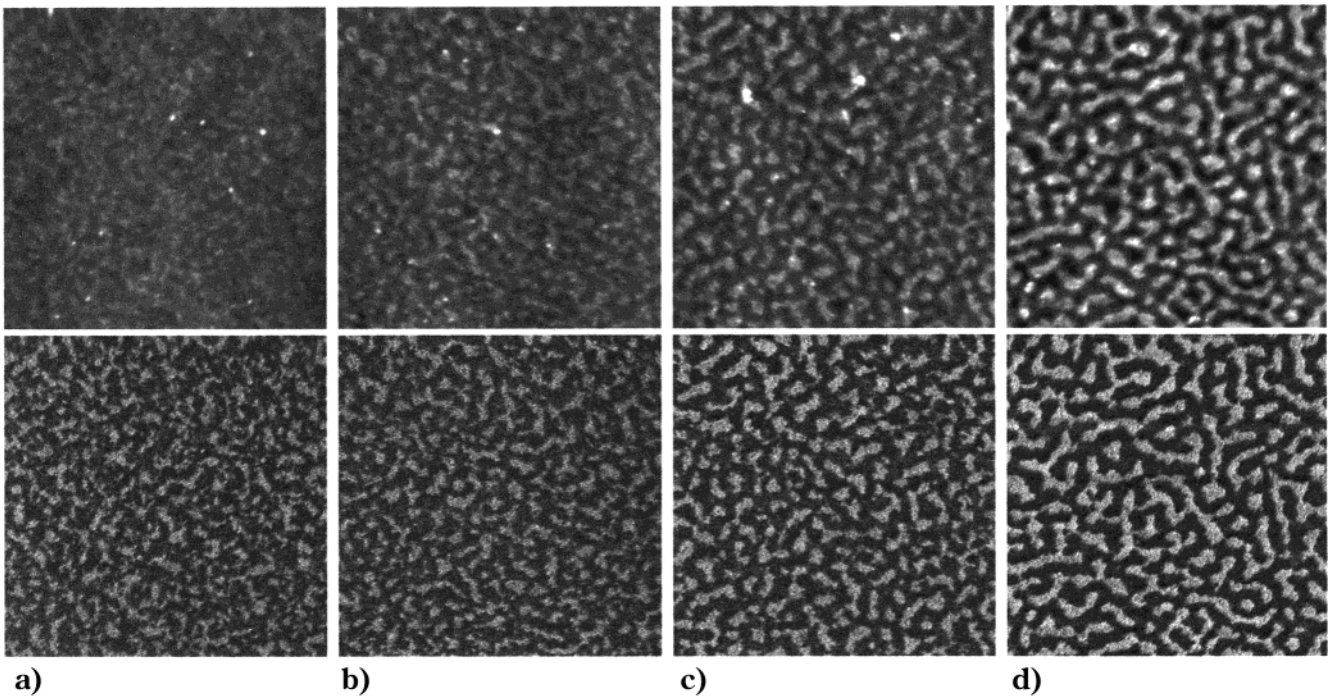

Figure 2. Topography (top) and phase contrast (bottom) of spin-case ultrathin films of SM120, dropping different concentrations at 4500 rpm. (a) 0.5, (b) 1.5, (c) 2.5, and (d) 3.5 g/L. Image size: 500 nm × 500 nm, height: 6 nm, phase shift: 8°.

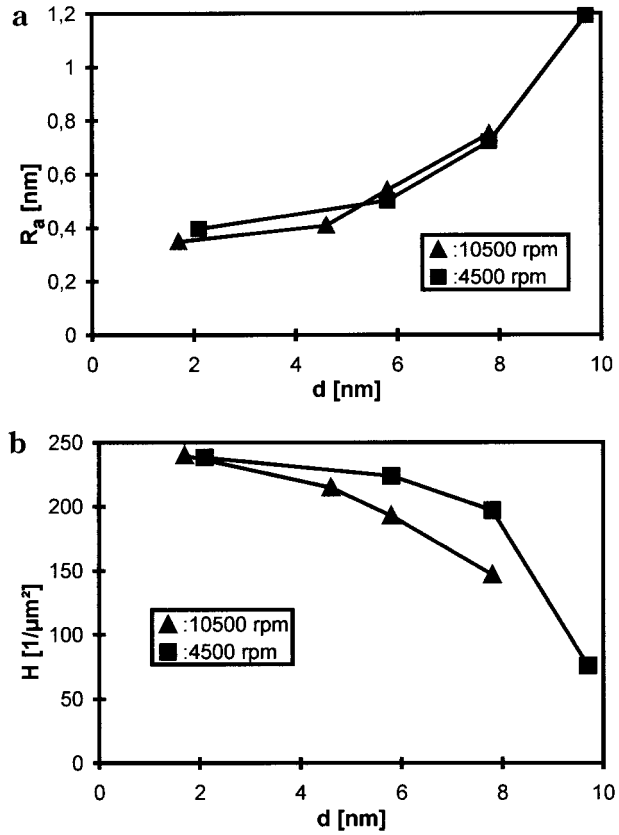

Figure 3. (a) Roughness (R_a) and (b) number (H) of PMMA microphases per area vs the film thickness (from Table 1).

films **b**, **c**, **h**, and **d** (Table 1) but after annealing do not show any differences when compared to the topography of film **g**. It can clearly be seen that the film topography with initial film thicknesses larger than 5.8 nm differs from that of the thinner ones.

To investigate the film morphology of these annealed ultrathin diblock copolymer films, the annealed film **a** was chosen for selective plasma etching and was compared with the annealed reference sample **f**. The two samples were measured by AFM choosing the same parameters (light tapping) taking height and phase shift simultaneously. The result is given in Figure 6, showing differences in the images of phase shift. These differences are caused by the etching process in which the PMMA blocks were removed, so that the topographical image of film **a** (Figure 6a) shows PS microdomains surrounded by the silicon substrate. In contrast, the topographical image of film **f** (Figure 6b) shows PS microdomains surrounded by a flat layer of PMMA (Figure 7a). This result is supported by the results of Spatz,[25,26] who investigated annealed samples of ultrathin poly(styrene-*block*-2-vinylpyridine) films on mica and is supported by measurements of harmonically modulated friction (HM-LFM)[19,20] at films **f** and **a**, showing that the etched film **a** has lost its anchorage to the substrate, so that the PS microdomains can be easily moved by the AFM tip, whereas the as-annealed film **f** can be depicted even with higher forces by HM-LFM.

In Figure 7a, the schematic side view of an annealed ultrathin diblock copolymer film with an initial thickness smaller than 5.8 nm is shown.

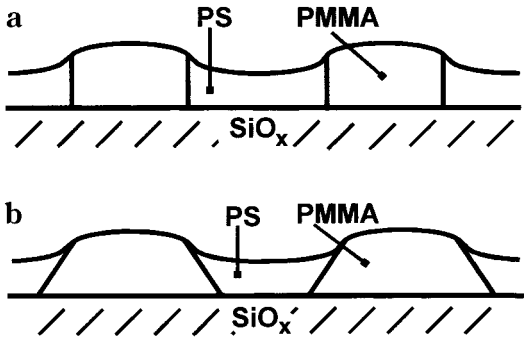

Figure 4. Schematic side view of two possible morphologies of spin-case diblock copolymer films on silicon substrate.

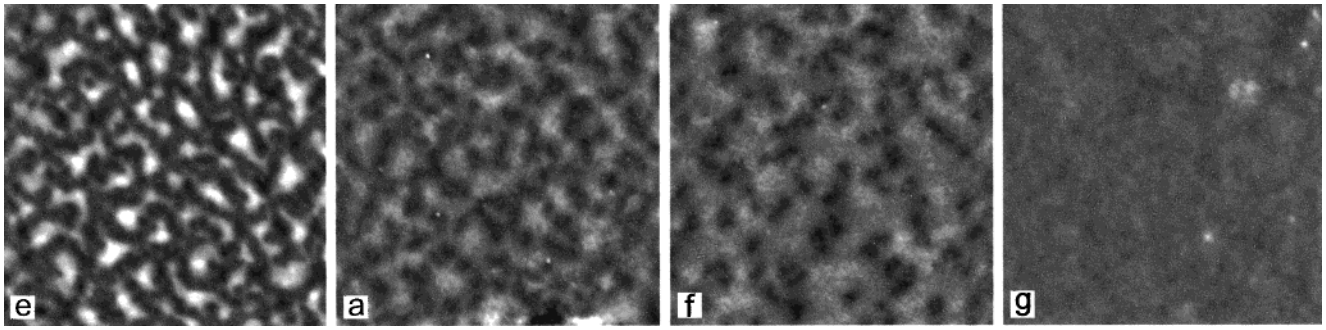

Figure 5. Topography of a selection of ultrathin SM120 diblock copolymer films after annealing at 130 °C. Initial film thicknesses: **e**: 1.8 nm; **a**: 2.1 nm; **f**: 4.6 nm; **g**: 5.8 nm. Image size: 1 μm × 1 μm; height: 7 nm.

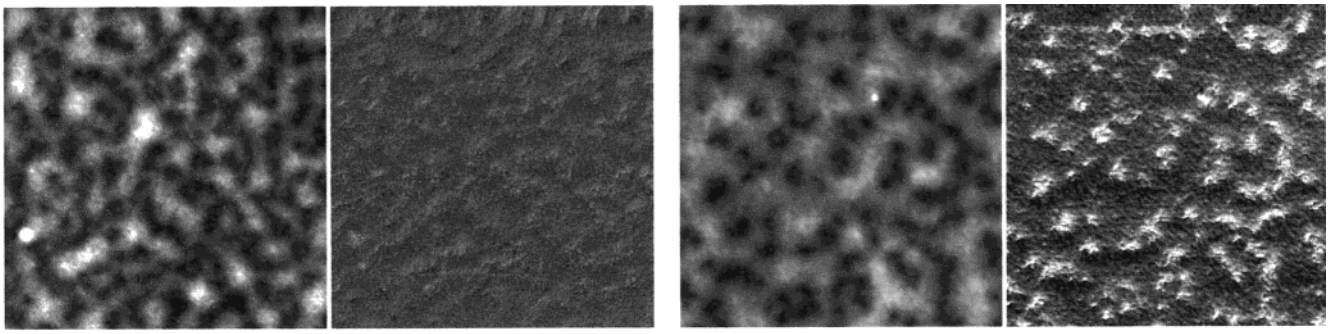

Figure 6. Topography (left) and phase contrast (right) (a) of the annealed film **a** after selective etching for 5 s with 40 W and (b) of the reference film **f** (annealed only). Image size: 1 μm × 1 μm; height: 8 nm; phase shift: 30°.

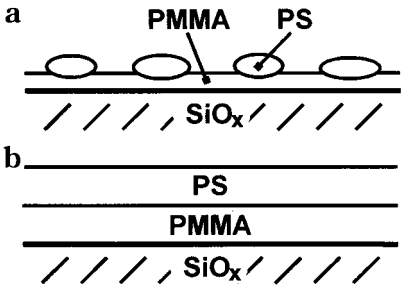

Figure 7. Schematic side view of annealed ultrathin diblock copolymer films with initial thickness (a) smaller and (b) larger than the minimum thickness of coplanar lamellar ordering.

Analogous to this result, the film morphology of the annealed films with initial thicknesses above 5.8 nm is clear: coplanar layers of PS and PMMA are hidden under the flat surface (Figure 7b). Because of its high interface energy, PMMA is able to lie flat on the silicon substrate, whereas PS needs more material to wet the PMMA layer completely.

Considering the interface thickness of PS and PMMA, the minimum film thickness of coplanar lamellar ordering in the SM120 diblock copolymer film is found to be about 40% higher than the calculated interface thickness in lamellar-ordered bulk material at 130 °C.[27−30]

Acknowledgment. The German National Science Found (DFG) has supported this work. We want to thank A. Lippitz, W. Unger, and U. Beck, Federal Institute for Materials Research and Testing (BAM) Berlin, for measuring the film thicknesses by ESCA and Ellipsometry, respectively. The cooperation and many discussions with H. Sturm, BAM, Berlin, are greatly appreciated. We gratefully acknowledge R. Stadler for providing the polymer samples.

References and Notes

(1) Anastasiadis, S. H.; Russel, T. P.; Satija, S. K.; Majkrzak, C. F. *Phys. Rev. Lett.* **1989**, *62*, 1852.
(2) Coulon, G.; Russell, T. P.; Deline, V. R.; Green, P. F. *Macromolecules* **1989**, *22*, 2581.
(3) Russell, T. P.; Coulon, G.; Deline, V. R.; Miller, D. C. *Macromolecules* **1989**, *22*, 4600.
(4) Anastasiadis, S. H.; Russell, T. P.; Satija, S. K.; Majkrzak, C. F. *J. Chem. Phys.* **1990**, *92*, 5677.
(5) Coulon, G.; Collin, B.; Ausserre, D.; Chatenay, D.; Russell, T. P. *J. Phys. (Paris)* **1990**, *51*, 2801.
(6) Maaloum, M.; Ausserre, D.; Chatenay, Coulon, G.; Gallot, Y. *Phys. Rev. Lett.* **1992**, *68*, 1575.
(7) Menelle, A.; Russell, T. P.; Anastasiadis, S. H.; Satija, S. K.; Majkrzak, C. F. *Phys. Rev. Lett.* **1992**, *68*, 67.
(8) Mayes, A. M.; Russell, T. P.; Bassereau, P.; Baker, S. M.; Smith, G. S. *Macromolecules* **1994**, *27*, 749.
(9) Collin, B.; Chatenay, D.; Coulon, G.; Ausserre, D.; Gallot, Y. *Macromolecules* **1992**, *25*, 1621.
(10) Russell, T. P.; Menelle, A.; Anastasiadis, S. H.; Satija, S. K.; Majkrzak, C. F. *Macromolecules* **1991**, *24*, 6263.
(11) Coulon, G.; Daillant, J.; Collin, B.; Banattar, J. J.; Gallot, Y. *Macromolecules* **1993**, *26*, 1582.
(12) Russell, T. P.; Hjelm, R. P.; Seeger, P. A. *Macromolecules* **1989**, *23*, 890.
(13) Magonov, S. N.; Elings, V.; Whangbo, M.-H. *Surf. Sci. Lett.* **1997**, *375*, L385.
(14) Löwenhaupt, B.; Hellmann, G. P. *Colloid Polym. Sci.* **1990**, *268*, 885.
(15) Löwenhaupt, B.; Hellmann, G. P. *Polymer* **1991**, *32*, 1065.
(16) Nick, L.; Kindermann, A.; Fuhrmann, J. *Colloid Polym. Sci.* **1994**, *272*, 367.
(17) Nick, L.; Lippitz, A.; Unger, W.; Kindermann, A.; Fuhrmann, J. *Langmuir* **1995**, *11*, 1912.
(18) Auschra, C.; Stadler, R.; Voigt-Martin, I. G. *Polymer* **1993**, *34*, 2094.
(19) Sturm, H. *Macromol. Symp.* **1999**, *147*, 249−258.
(20) Sturm, H.; Schulz, E.; Munz, M. *Macromol. Symp.* **1999**, *147*, 259−267.

(21) Binder, K. *Adv. Polym. Sci.* **1999**, *138*, 1.
(22) Brandrup, J.; Immergut, E. H. *Polymer Handbook*, 3rd ed.; Wiley Publication: New York, 1991.
(23) Baschnagel, J.; Binder, K. *Macromolecules* **1995**, *28*, 6808.
(24) Han, C. C.; Mozer, B. *Macromolecules* **1977**, *10*, 44.
(25) Spatz, J. P.; Sheiko, S.; Möller, M. *Adv. Mater.* **1996**, *8*, 513.
(26) Spatz, J. P.; Möller, M.; Noeske, M.; Behm, R. J.; Pietralla, M. *Macromolecules* **1997**, *30*, 3874.
(27) Helfand, E.; Wasserman, Z. R. Ref 7, Seite 99. In Goodman, I. *Developments in Block Copolymers-1;* Applied Sci.: New York, 1982.
(28) Callaghan, T. A.; Paul, D. R. *Macromolecules* **1993**, *26*, 2439.
(29) Russell, T. P. *Macromolecules* **1993**, *26*, 5819.
(30) Russell, T. P.; Chin, I. *Colloid Polym. Sci.* **1994**, *272*, 1373.

MA001288F